Temperature-dependent regulation of the *Escherichia coli lpxT* gene

Barbara Sciandrone[a,1], Francesca Forti[a], Sara Perego[a], Federica Falchi[a], Federica Briani[a,#]

[a]Dipartimento di Bioscienze, Università degli Studi di Milano, Italy

[1]Present address: Dipartimento di Biotecnologie e Bioscienze, Università degli Studi di Milano-Bicocca, Italy

Running Head: Temperature-dependent regulation of the *E. coli lpxT* gene

[#]Address correspondence to Federica Briani, federica.briani@unimi.it

ABSTRACT

The Lipid A moiety of the lipopolysaccharide can be covalently modified during its transport to the outer membrane by different enzymes, among which the LpxT inner membrane protein. LpxT transfers a phosphate group from the undecaprenyl pyrophosphate to the Lipid A, a modification affecting the stability of the outer membrane and its recognition by the host immune system in Enterobacteria. We previously found that the expression of the *Pseudomonas aeruginosa lpxT* gene, encoding LpxT, is induced in response to a temperature upshift and we proposed that an RNA thermometer was responsible for such regulation. Here we show that the *Escherichia coli lpxT* orthologous gene is down-regulated upon a temperature upshift and investigated the mechanism of this regulation. We found that the LpxT protein stability is not affected by the temperature change. Conversely, the *lpxT* mRNA levels strongly decrease upon a shift from 28 to 42 °C. The lack of MicA sRNA, which was previously implicated in *lpxT* regulation, does not affect *lpxT* thermal regulation. We identified the *lpxTp* promoter and demonstrated that *lpxTp* has temperature-sensitive activity depending on its peculiar -10 region. Moreover, we found that RNase E-dependent degradation of the *lpxT* mRNA is also modulated by temperature causing a strong destabilization of the *lpxT* mRNA at 42 °C. *In vitro* data argue against the involvement of factors differentially expressed at 28 and 42 °C in the temperature–dependent modulation of *lpxT* mRNA stability.

1. INTRODUCTION

The outer membrane (OM) of Gram negative bacteria is composed by an internal phospholipidic (PL) leaflet and an external layer consisting of a tight array of lipopolysaccharide (LPS) molecules. The LPS is a complex amphipathic glycolipid composed by Lipid A, which is the LPS hydrophobic moiety facing the PL layer, and an oligosaccharide core, which can be linked to the O-antigen, a polysaccharide chain of variable length facing outwards [1]. The Lipid A, or endotoxin, is the LPS most conserved part. In *Escherichia coli*, the Lipid A is typically composed by a dimer of β-1'-6-linked glucosamine residues phosphorylated at the 1 and 4′ positions, to which six fatty acyl chains are attached. Specific enzymes can extensively modify the Lipid A by changing the number of acyl chains and by linking additional phosphate groups or small molecules like phosphoetanolammine (pEtN) and 4-amino-4-deoxy-L-arabinose (L-Ara4N) to the glucosamine dimer. Such modifications have an impact not only on the OM stability and rigidity, but also on the interaction between the LPS and molecules of the innate immune response. A variety of environmental stimuli, among which temperature changes, control the Lipid A modification pattern [2,3]. For instance, pathogenic bacteria like *Francisella tularensis* or *Yersinia pestis* exploit the mammalian host body temperature as a signal to modulate the acylation degree of their Lipid A [4,5]. Lipid A phosphorylation is also controlled by temperature in different bacteria. Indeed, in the psychrotrophic bacterium *Pseudomonas syringae,* the LPS is phosphorylated on both the Lipid A and core oligosaccharide in response to a temperature upshift (from 0 to 22 °C) [6]. Moreover, in *Porphyromonas gingivalis,* a bacterium evolutionarily very distant from both *Pseudomonas* and *E. coli,* Lipid A phosphorylation increases upon a small temperature rise (from 37 to 40 °C) [7]. Thus it seems that bacteria thriving in different environments and with disparate lifestyles may benefit from thermal modulation of Lipid A phosphorylation.

In a previous work, we reported the identification of *lpxT* among *P. aeruginosa* genes up-regulated at post-transcriptional level by a temperature increase from 25 to 37 °C [8]. The *lpxT* gene encodes an inner membrane protein belonging to the class of acidic phosphatases that is responsible for Lipid A phosphorylation in both *P. aeruginosa* and *E. coli* [9,10]. Undecaprenyl pyrophosphate, a phosphorylated derivative of the essential transporter of cell wall components undecaprenyl phosphate, is the phosphate donor in the reaction catalyzed by LpxT [3,9]. *P. aeruginosa* LpxT phosphorylates the Lipid A at either of two sites (e.g. at the 1 and 4' positions) [10], whereas the *E. coli* LpxT orthologous protein phosphorylates the Lipid A only at the 1-position [9]. This modification is abundant in *E. coli*, as about one third of Lipid A has a pyrophosphate group at that position [11].

In this study, we investigated whether the *E. coli lpxT* gene is also regulated in a temperature-dependent manner. We found that LpxT abundance decreases in cells acclimated at high temperature. Consistent with this finding, we observed that both transcription from the *lpxTp* promoter and *lpxT* mRNA stability are down-regulated by a temperature upshift, strongly decreasing the amount of *lpxT* mRNA. Our data demonstrate that transcriptional regulation depends on intrinsic features of the *lpxT* promoter and that temperature-dependent cleavage(s) by RNase E modulates *lpxT* mRNA stability.

2. RESULTS

2.1 LpxT expression is down-regulated at high temperature

In order to test whether the expression of the *E. coli lpxT* gene is modulated by temperature, we analyzed the production of the LpxT protein at different temperatures. To this aim, since LpxT-specific antibodies were not available, we tagged the *lpxT* open reading frame (ORF) in the BW25113 strain with a GFP reporter gene inserted into the chromosome immediately before the

lpxT stop codon (strain KG273; Table 1). LpxT$_{GFP}$ chimeric proteins with the GFP C-terminally fused to LpxT had been previously shown to be inserted into the inner membrane and absent in soluble protein fraction [12,13]. We analysed membrane proteins of both the recombinant strain and the parental BW25113 grown at 28 °C and shifted to 37 and 42 °C. Western blotting with GFP-specific antibodies showed a single band present in the *lpxT-GFP* recombinant strain and absent in BW25113 (Fig. 1A). The apparent molecular weight (MW) of LpxT$_{GFP}$ was lower than the formula MW (i.e.54 kDa), a feature previously reported for an LpxT$_{GFP}$ fusion constructed by another research group [12] and common among membrane proteins [14]. 20 min after the shift from 28 °C to higher temperatures, LpxT$_{GFP}$ was similarly abundant at 28 and 42 °C and slightly increased at 37 °C. After longer incubation (i.e. 60 min after the shift), the LpxT$_{GFP}$ signal was stronger at 28 °C than at 37 and 42 °C (Fig. 1A).

To assess whether down-regulation of *lpxT* expression may depend on differential transport to the inner membrane at different temperatures, we analysed whole cell lysates of the *lpxT-GFP* strain grown at 28 and 42 °C by Western blot with the GFP antibody. Unfortunately, we could not get reliable results because the GFP antibody gave many unspecific signals when probed on total proteins (data not shown). To overcome this problem, we constructed a recombinant BW25113 derivative carrying a fusion between *lpxT* and the sfGFP, a GFP variant with increased fluorescence [15]. This allowed to visualize the chimeric LpxT$_{sfGFP}$ protein as a fluorescent band in polyacrylamide gels. Consistent with what already observed for LpxT$_{GFP}$ in the membrane fraction, LpxT$_{sfGFP}$ amount in whole cell extracts was reduced at high temperature (Fig. 1B), ruling out differential protein transport at 28 *vs.* 42 °C as the source of the temperature effect on the *lpxT* expression pattern.

As *lpxT* was reported among putative targets of the MicA small RNA (sRNA) [16], we tested whether MicA was involved in temperature-dependent regulation of *lpxT* expression by analysing the effect of *micA* deletion on the expression of *lpxT*-sfGFP at 28 and 42 °C. As shown in Fig. 1B,

the mutation did not affect *lpxT*-sfGFP expression profile at the two temperatures, indicating that MicA does not play a significant role in temperature-dependent *lpxT* regulation.

2.2 LpxT stability is not regulated by temperature

Decreased LpxT amount at 42 °C could be due to protein destabilization at high temperature. To test this hypothesis, we analysed the stability of LpxT$_{sfGFP}$ by assaying the amount of protein remaining after protein synthesis inhibition with chloramphenicol. LpxT$_{sfGFP}$ resulted to be stable at all tested temperatures (half-life≥ 90 min at 28 and 42 °C; Fig. 1C), arguing against the hypothesis that LpxT protein stability may be regulated by temperature.

2.3 The *lpxT* mRNA amount is decreased at high temperature

To assess whether the *lpxT* expression profile at different temperatures may depend on thermal transcription regulation, we analyzed *lpxT* locus transcription in the *lpxT*$^+$ BW25113 strain. Previous work had located the *E.coli lpxTp* promoter in the 250 bp region upstream of the *lpxT* ORF, suggesting that the *lpxT* gene could be transcribed as a monocistronic mRNA [12]. By primer extension with an *lpxT* specific oligonucleotide, we identified a single mRNA 5'-end mapping 28 nt upstream of the *lpxT* ORF start codon (i.e. at G2268826). The mRNA signal was detectable in exponential cultures and absent in stationary phase (Fig. 2A). A faint signal compatible with a monocistronic mRNA ca. 800 nt long was observed in Northern blotting experiments with an *lpxT*-specific riboprobe. The *lpxT* signal was clearly more abundant at low temperature than after a 15 min shift to 37-42 °C (Fig. 2B; see t=0 samples in Fig. 2C). Change in *lpxT* mRNA amount was fast, as it was already evident 5 min after shifting the bacterial cultures from 28 to 42 °C (Supplementary Fig. S1). Transcription of the *lpxT-GFP* locus in the KG-273 strain showed a similar pattern, with a single signal corresponding to a monocistronic mRNA more abundant at 28 than at 37-42 °C (see t=0 samples in Fig. 2D).

2.4 The *lpxTp* promoter activity is down-regulated at high temperature

To investigate whether temperature influenced the efficiency of transcription initiation at the *lpxTp* promoter, we cloned upstream of the GFP reporter gene a 49 bp long DNA fragment corresponding to the region immediately upstream of the *lpxT* transcription start site (TSS) mapped by primer extension (plasmid pLPXTp; Fig. 3A). Such region was previously demonstrated to contain the *lpxTp* promoter in the *Salmonella enterica lpxT* orthologous gene [17]. The presence of the 49 bp long DNA fragment was sufficient to boost the expression of the GFP reporter gene and promoted the production of a transcript whose 5'-end corresponds to the natural TSS of the *lpxT* mRNA (Figs. 3B and 3C). Thus the short region cloned in pLPXTp contains the *E. coli lpxTp* promoter. Moreover, we found that the fluorescence of the cultures carrying pLPXTp was almost twofold higher at 28 than at 42 °C. To test whether this may depend on temperature affecting *lpxTp* activity, we measured the amount of GFP mRNA produced in cells carrying pLPXTp at 28 and 42 °C by RT-qPCR. As shown in Fig. 3D, the mRNA was ca. two-fold more abundant at 28 °C than at 42 °C, suggesting that *lpxTp* may be more active at low temperature.

By examining the sequence of the *lpxTp* promoter, we noticed that it bears a -10 region (i.e. TAAGGT) present in a small number of *E. coli* promoters, among which the σ^D-dependent promoter of the *dsrA* gene. It was shown that *dsrA* transcription is temperature-sensitive and that mutations in the -10 abolish the thermal response [18]. To assess whether *lpxTp* was similarly regulated, we replaced the natural -10 of *lpxTp* with the σ^D consensus sequence (i.e. TATAAT) in the reporter construct and quantified by RT-qPCR the GFP mRNA at 28 and 42 °C. The mutation abolished the thermal sensitivity of *lpxTp*, as the mRNA amount at the two temperatures was not significantly different (Fig. 3D), thus confirming that the -10 is a thermo-sensitivity determinant for *lpxTp*.

2.5 The stability of the *lpxT* mRNA is affected by temperature

The *lpxT* and *lpxT-GFP* mRNAs seemed to be more stable at 28 °C than at 37-42 °C (Figs. 2C and 2D). However, while we could measure their half-lives (HL) at 28 °C (Table 2), the low abundance of the two transcripts at high temperature hampered precise HL determination at 42 °C. To circumvent this problem, we cloned the *lpxT* gene with its natural leader region and the 170 bp downstream under the transcriptional control of the *araBp* promoter in a multicopy vector (plasmid pLPXT; Fig. 4A). Transcription from *araBp* should produce an *lpxT* mRNA almost identical to the natural one, with only an extra nucleotide at the 5'-end. The expression and stability of the *lpxT* transcript at 28 and 42 °C were analysed by Northern blotting (Fig. 4B). Upon arabinose addition to the cultures, we observed two signals corresponding to an RNA ca. 800 long, similar to the *lpxT* mRNA transcribed from the chromosomal locus, and a longer mRNA, which likely terminates downstream of the cloned region. Both *lpxT* transcripts transcribed from the plasmid were more stable at low temperature, with an HL of around 3 min at 28 °C and of *ca.* 1 min at high temperature (Fig. 4B and Table 2), showing that the *lpxT* mRNA is destabilized by a temperature upshift. We measured also the HL of an *lpxT* mRNA variant lacking the natural 3'-UTR region (i.e. the *lpxT$_{HA}$* mRNA deriving from plasmid pLPXTHA; Fig. 4A) and also in this case we observed that the transcript was more stable at 28 than at 42 °C (Fig. 4C and Table 2).

In spite of faster decay, the *lpxT* mRNAs transcribed from pLPXT and pLPXTHA were more abundant after a 10 min shift from 28 to 42 °C (Figs. 4B and 4C), suggesting that transcription from the *araBp* promoter may be more active at high temperature and compensate for *lpxT* mRNA destabilization. In agreement with this hypothesis, we found that an *lpxT*-sfGFP fusion integrated into the chromosome at the *araB* locus was up-regulated at the transcriptional level at 42 °C (Supplementary Fig. S2). Increased expression at 42 °C was observed also for a *recA*-sfGFP reporter gene (i.e. the sfGFP ORF fused with the leader region and the first 8 codons of the *recA* gene) integrated into the same locus, showing that this effect is not specific for *lpxT* or *lpxT-*

containing chimeric genes and thus probably depends on enhanced transcription from *araBp* at high temperature.

2.6 RNase E is responsible for efficient degradation of the *lpxT* mRNA at high temperature

In *E. coli*, mRNA decay is often initiated by an endonucleolytic cut performed by RNase E [19]. To assess whether RNase E participates also in *lpxT* mRNA degradation at high temperature, we measured the stability at 42 °C of the *lpxT* mRNA transcribed from pLPXT in the C-5868 strain, which carries the *rne-131* allele encoding a thermosensitive (*ts*) RNase E, and in the isogenic C-5869 *rne*+ strain. As a control, *lpxT* mRNA HL in the *rne*+ strain at 28 °C was also measured. In the *rne*+ strain, we observed that the HL of the *lpxT* mRNA was ca. 4 min and 1 min at 28 and 42 °C, respectively, in agreement with the results obtained in BW25113. The *rne* mutation strongly stabilized *lpxT* mRNA at high temperature, as the HL was about 3 min in the *rne ts* strain (Table 2 and Fig. 4D), indicating that RNase E plays a major role in efficient *lpxT* mRNA degradation at high temperature.

2.7 Differential degradation of the *lpxT* mRNA 5'-end region does not require factors endowed with temperature-dependent expression

To assess whether *trans*-acting factors induced by the temperature upshift are responsible for thermal regulation of *lpxT* mRNA decay, we assayed *in vitro* degradation of a radiolabeled RNA probe corresponding to the first 80 nt of the *lpxT* transcript (LPXT probe) at 28 and 42 °C. This portion of the transcript contains three occurrences of the RNWUU motif (with R as G/A, W as A/U, and N as any nucleotide; Supplementary Fig. S3A), which was identified as the consensus sequence for RNase E cleavage [20]. The probe was incubated with total extracts of *E. coli* cultures grown at either 28 and 42 °C. After 10 min, the reactions were stopped and loaded on a polyacrylamide gel to visualize the LPXT probe signal. Irrespective of the temperature at which the

cultures for extract preparation were grown, the LPXT signal was undetectable in all samples incubated at 42 °C and signals corresponding to short degradation fragments were visible. Conversely, the LPXT signal was present in the samples incubated at 28 °C (Fig. 5A). In principle, both endonucleolytic cleavage or exonucleolytic degradation from the 3'-end could be responsible for LPXT degradation at 42 °C. However, protection of the 3'-end of the RNA probe through pairing with a complementary 20 nt long oligonucleotide (primer 3332) did not prevent LPXT degradation at 42 °C (Fig. 5B), suggesting that the riboprobe decay is mainly due to endonucleolytic cut(s). To assess whether RNase E was involved in LPXT degradation, extracts of the *E. coli rne* ts mutant and its isogenic *rne*[+] strain were incubated at 42°C with LPXT. As shown in Fig. 5B, the LPXT probe was completely degraded upon incubation with the *rne*[+] extract, whereas a signal corresponding to the full length probe was still present, albeit faint, upon LPXT incubation with the *rne-131* extract, suggesting that RNase E is involved in *in vitro* degradation of LPXT. To strengthen such conclusion, we probed the effect on LPXT stability of the *E. coli* RNA degradosome, a multicomponent complex assembled on RNase E and including the exonuclease PNPase, the RNA helicase RhlB, and the metabolic enzyme enolase [21]. The complex between the LPXT probe and the oligonucleotide 3332 was incubated with the RNA degradosome in conditions in which the exonucleolytic activity of PNPase was not active (i.e. without adding orthophosphate in the reaction mix [22]). We found that the signal corresponding to the full length LPXT decreased with time at both 28 and 42 °C, with degradation being slightly (but reproducibly) more efficient at 42°, and signals corresponding to shorter RNAs slowly increased (Fig. 5C), in agreement with the hypothesis that *in vitro* degradation of LPXT relies on the endonucleolytic activity of RNase E.

3. DISCUSSION

Lipid A modifications that impact on OM fluidity and permeability are regulated by temperature in distantly related bacteria [4,23–25]. Experimental evidence presented in this study shows that the *E. coli lpxT* gene is down-regulated when cells are exposed to a temperature upshift, suggesting that

phosphorylation of Lipid A may depend on environmental temperature. We investigated the mechanisms that link *lpxT* expression to temperature. We observed that the amount of LpxT$_{GFP}$ protein is decreased at 42 °C, although the protein remains stable at high temperature, with an HL higher than 90 min. This rules out the hypothesis that the protein may become per se more susceptible to proteases at high temperature and/or that it could be degraded by proteases induced at 42 °C. On the other hand, we observed that both the *lpxT*$^+$ and the *lpxT*-GFP mRNA become scarce after a temperature upshift. Thus, the LpxT protein drops in cells acclimated at high temperature because the cognate mRNA amount is decreased and the extant protein is diluted due to cell growth and division. It is interesting that in the acclimation phase (i.e. 20 min after the temperature upshift), in spite of the quick drop in the mRNA levels, the LpxT$_{GFP}$ protein amount slightly increased (at 37 °C) or remained unchanged (at 42 °C). We are currently investigating the mechanism transiently uncoupling mRNA and protein production. It is possible that the efficiency of *lpxT* mRNA translation may increase at high temperature, partially compensating for its reduced amount. Our data show that both mRNA synthesis and degradation are regulated by temperature-responsive mechanisms. At low temperature, the *lpxTp* promoter is active and the *lpxT* mRNA is relatively stable. Upon a temperature upshift, both *lpxTp* promoter activity and *lpxT* mRNA stability decrease, leading to a fast decline of the *lpxT* mRNA cellular content. In stationary cultures, irrespective of the temperature, the *lpxTp* activity is reduced (see Figs. 2A and 3C; data not shown), a feature common to many σ^D dependent promoters [26]. We have identified an *in cis* element involved in thermal regulation of transcription initiation from *lpxTp*. Indeed, *lpxTp* has a peculiar -10 TAAGGT hexamer, which is present also in the promoter of the DsrA sRNA gene. Mutating the -10 abolishes thermoregulation of both *dsrAp* [18] and *lpxTp*. It has been hypothesized that the TAAGGT hexamer may make *per se* the *dsrA* transcription temperature-sensitive, without the intervention of *trans*-acting factors [18]. However, our data do not rule out the possibility that a repressor expressed or active only at high temperature may recognize such sequence in *lpxTp*. On the other hand, the *lpxTp* promoter has not a recognizable properly-spaced -35 element, whereas a -35 region

separated by a 17 bp long spacer from the TAAGGT -10 was demonstrated to be strictly required for initiation from the *dsrA* promoter [18]. This suggests that efficient transcription initiation from *lpxTp* may need an activator. Indeed, a putative binding site for the PhoP response regulator is located in position -26 to -42 with respect to the TSS and PhoP-dependent induction of *lpxT* transcription at low Mg^{2+} concentration (i.e. the activating condition for the PhoPQ two-component system) has been found both in *E. coli* and *Salmonella enterica* [17]. Interestingly, the two regulatory elements identified in the *E. coli lpxTp* promoter (i.e. the PhoP binding site overlapping the -35 region and the TAAGGT hexamer at -10) are both conserved in promoters of the *lpxT* orthologs of *S. enterica*, *Klebsiella pneumoniae* and *Citrobacter freundii* [17], suggesting that also in these bacteria *lpxT* transcription may be regulated by both temperature and Mg^{2+} concentration. In *E. coli*, *phoP* expression is negatively modulated by MicA sRNA [27], suggesting that MicA could act as an indirect negative regulator of *lpxT* transcription. In fact, decreased *lpxT* mRNA amount upon MicA over-expression from a plasmid was reported [16]. However, we did not detect any significant *lpxT* expression change at different temperatures in a Δ*micA* strain, suggesting that MicA sRNA may have only a marginal role, if any, in regulating *lpxT* expression in our experimental settings.

We showed that besides *lpxT* mRNA synthesis, also its stability is regulated by temperature. At high temperature, the *lpxT*, *lpxT*-GFP and *lpxT*$_{HA}$ mRNAs, which have almost identical 5'-ends and differ at their 3'-ends, are all destabilized, indicating that the *in cis* determinants of thermoregulation do not lie within the mRNA 3'-UTR. Consistent with these results, we found that the LPXT RNA probe corresponding to the first portion of the *lpxT* transcript was completely degraded upon in *vitro* incubation at 42 °C with *E. coli* extracts, whereas the probe remained stable at 28 °C. A mutation inactivating RNase E affected cleavage both *in vivo*, causing a ca. threefold increase in *lpxT* mRNA HL at 42 °C, and to a certain extent also *in vitro,* supporting the idea that RNase E is responsible for efficient *lpxT* mRNA degradation at 42 °C. Consistently, LPXT is degraded *in vitro* by the RNase E-based RNA degradosome generating a reproducible pattern of

RNA fragments compatible with multiple endonucleolytic cuts. However, the *rne ts* mutation only moderately interferes with *in vitro* LPXT degradation in whole extracts. Partial RNase E inactivation at 42 °C and/or the intervention of other nucleases, like for instance RNase G, an RNase E homolog with similar cleavage site specificity [19] may explain LPXT decay upon incubation with the *rne ts* extract.

It remains to be established how cleavage by RNase E of *lpxT* mRNA may be modulated by temperature. The LPXT probe is stable when incubated at 28 °C with cell extracts, whereas it is promptly degraded at 42 °C irrespective of the temperature at which the cultures for extract preparation were grown. Thus, it seems that temperature-dependent *lpxT* mRNA degradation does not require the induction of factors differentially expressed at different temperatures. On the other hand, the RNA degradosome purified from *E. coli* cultures grown at 37 °C is able to degrade the LPXT probe also at 28 °C, suggesting that a *trans*-acting factor present in whole cell extracts and absent in the RNA degradosome preparation may prevent LPXT degradation at 28 °C. This factor could preclude the cleavage of the probe either directly, by binding the RNase E cleavage site(s) at low temperature, or indirectly, for instance by stabilizing inhibitory secondary structure(s) formed by the *lpxT* mRNA. Indeed, the 5'-UTR of the *lpxT* mRNA has the potential to fold into a relatively unstable stem-loop (predicted ΔG of -4.3 kcal/mol at 28 °C; Supplementary Fig. S3A), which could potentially interfere with RNase E-dependent degradation by sequestering the 5'-end of the transcript at low temperature [19].

Notably, in both chromosomal and plasmid constructs, when the *lpxTp* promoter is replaced by *araBp*, the *lpxT* mRNA level increases at 42 °C, suggesting that transcription from the *araBp* promoter may be up-regulated by temperature and counteract *lpxT* mRNA destabilization. Since the *araBp* promoter is largely used in expression systems and in reporter constructs, it would be interesting to clarify to which extent its activity is actually temperature-dependent.

In order to fully understand the physiological meaning of *lpxT* thermal regulation, it will be important to assess how it is integrated with other known regulatory mechanisms like negative

regulation of LpxT activity by the PmrAB two component system [12,17]. In the presence of a PmrB-activating stimulus like high Fe^{3+}, PmrA promotes the transcription of the genes coding for PmrR - a short polypeptide inhibiting LpxT activity [28]- and for ArnT and EptA, two enzymes that modify the Lipid A by introducing the positively charged residues phosphoetanolammine (pEtN) and 4-amino-4-deoxy-L-arabinose (L-Ara4N). The introduction of positive charges into Lipid A decreases the OM affinity for PmrB-activating Fe^{3+} and this relieves LpxT inhibition [3,28]. Such feedback loop causes a continuous remodeling of Lipid A modification. This is particularly relevant for bacteria thriving in mammalian intestine, in which both bile salts and antimicrobial peptides (AMPs) are present, as positive charges on Lipid A decrease the resistance towards anionic detergent like the bile component deoxycholic acid, but they increase the resistance towards AMPs [29,30]. Since LpxT inhibits EptA-dependent modification [12], *lpxT* down-regulation in cells acclimated at the mammalian host temperature may represent a mechanism to enhance resistance to AMPs by allowing the introduction of pEtN on Lipid A.

In *P. aeruginosa,* translation of the *Pa lpxT* mRNA appears to be induced upon a temperature upshift [8]. On the other hand, the *Pa lpxTp* promoter has an AT-rich -10 with a properly spaced -35 box similar to that of canonical σ^D promoters (Supplementary Fig. S3B), suggesting that transcription initiation should not be temperature-responsive in this bacterium. In fact, we found that the *Pa lpxT* mRNA is equally abundant at all temperatures [8]. Moreover, a PhoP binding site was not identified in *Pa lpxTp* promoter [17], implying that *Pa lpxT* transcription responds to stimuli other than those that govern transcription of the *E. coli* ortholog. It is interesting that also regulation of the *eptA* gene largely differs in *P. aeruginosa* and *E. coli* [31], suggesting that the two bacteria have evolved peculiar strategies to modulate in a coordinated way genes involved in Lipid A modification.

4. MATERIALS AND METHODS

4.1 Bacterial strains and plasmids

Bacterial strains and plasmids used in this study are listed in Table 1 and the oligonucleotides in Supplemental Table S1. *E. coli* genome coordinates throughout this work refer to MG1655 strain, Genbank Accession Number U00096.3. Strains with chromosomal insertions were constructed following the procedure described by Datsenko and Wanner (2000) [32]. In particular, to construct KG-273 (i.e. BW25113 *lpxT-GFP*), four DNA fragments were synthesized by PCR, corresponding to i) *lpxT* regions I (2269401-2269564) and II (2269568-2269738). The two fragments were obtained by amplification of MG1655 chromosomal DNA with oligonucleotides 3358-3359 and 3363-3364, respectively; ii) the eGFP coding region, obtained by PCR with primers 3360-3373 on pGM963 [33]; iii) the FRT-*kan*^{R}-FRT region, obtained by amplifying plasmid pKD13 [32] DNA with primers 3374-3362. In the second step, the partially overlapping fragments i) *lpxT* I and eGFP and ii) *kanR* and *lpxT* II were used as templates in two PCR reactions with oligonucleotides 3358-3373 and 3374-3364, respectively. Finally, the full length cassette was obtained by amplification of the two *lpxT* I-eGFP and *lpxT* II-*kanR* fragments with primers 3358-3364 and was integrated in BW25113/pKD46 by λ Red-mediated homologous recombination [32], obtaining strain BW25113 *lpxT*-GFP:*kan*. The *kan* cassette was excised from the recombinant strain by FLP-mediated recombination, obtaining KG-273. The LpxT-GFP protein expressed by KG-273 carries the Pro to Gln substitution in position 75 of the eGFP moiety (P42212 entry in www.uniprot.org/uniprot/) of the chimeric protein. KG-276 was constructed by transformation of BW25113/pKD46 with an sfGFP- *kan*^{R}-cassette with ends homologous to regions 2269515-2269563 and 2269617-2269568. The cassette was constructed by PCR amplification of sfGFP gene from pXG-10SF [15] and the *kan* resistance gene from pKD13 plasmids [32] with primers 3460-3461 and 3462-3463, respectively. The two fragments were used as DNA templates in a PCR reaction with 3460-3463 primers, which contained homology regions with the *lpxT* locus at their 5'-ends, generating the cassette used for transformation. The *kan* resistance gene was excised from the recombinant strain

by FLP-mediated recombination [32]. FLP-mediated recombination was used also to remove the chloramphenicol resistance gene from the DMEG3 strain [34], obtaining KG-279. KG-280 and KG-283 were obtained by transformation of KG-279/pKD46 with DNA fragments obtained by *Sma*I-*Eco*RV digestion of pGM2107 and pGM2109, respectively. KG-289 was obtained by P1 transduction of Δ*micA*:*tetR* from MG1449 [27] into KG-276. *Plasmid construction.* pLPXTHA was obtained as follows. The HA coding region was obtained by annealing oligonucleotides 3257-3258 and cloning the double stranded oligonucleotide in pGM930 between *Kpn*I and *Pst*I sites [8], obtaining plasmid pGM2035. The *lpxT* locus was PCR-amplified with oligonucleotides 3225-3273 (region 2268826-2269564; *lpxT* fragment) or 3286-3273 (regions 1020995-1020975 + 2268846-2269564; *recA-lpxT* fragment) on MG1655 genomic DNA. The *recA-lpxT* fragment was digested with *Nco*I-*Eco*RI and cloned in pGM2035 cut with the same enzymes, obtaining pGM2049. pLPXTHA was obtained by cloning the *lpxT* PCR fragment digested with *Pvu*II-*Eco*RI in pGM2049 digested with the same enzymes. pLPXT was obtained by replacing the *Pst*I-*Hind*III region of pLPXTHA with a DNA fragment obtained by PCR on BW25113 chromosomal DNA with the oligonucleotides 3475-3473. pGM2096 is a pLPXTHA derivative in which the HA epitope was replaced with the sfGFP gene (cloned in frame with *lpxT*) amplified by PCR on pXG-10SF [15] with the oligonucleotides 3476-3477. pGM2107 and pGM2109 were constructed by cloning in the *Sma*I site of pGM2096 and pGM2016 [8], respectively, a DNA fragment obtained by PCR on pKD3 [32] with the oligonucleotides 1669-3560. The plasmids were checked by sequencing. A 3 bp deletion overlapping the *Pvu*II site (causing the deletion of L_{108} in LpxT) was detected in pLPXTHA; the mutation maps in one of the transmembrane domain of the protein [13] and according to Phobius analysis (not shown), it does not change the overall hydrophobicity profile and predicted topology of the protein. Plasmids carrying transcriptional fusions were obtained as pGZ119EH derivatives [35]. First we cloned the *recA*-sfGFP reporter construct (obtained by PCR amplification of pGM2016 with primers 2804-3274) between the *Eco*RI and *Pst*I sites obtaining pGM2040. The pTAC promoter upstream of the reporter construct was either deleted by *Eco*RI-

*Eco*RV digestion, Klenow treatment and ligation, obtaining pGM2054, or replaced with a PCR fragment amplified from *lpxT* locus, namely region 2268778-2268826 (-49 to -1 relative to the *lpxT* mRNA 5'-end; primers 3281-3282), obtaining plasmid pLPXTp. pLPXTpmut carries the same region with the substitution of the -11/-9 AGG sequence with TAA. The mutagenized fragment was obtained by overlapping PCR with proper oligonucleotides and inserted between *Eco*RI-*Eco*RV sites of pGM2040.

Bacterial cultures were grown in LD [36]. When needed, media were supplemented as follows: 100 µg/ml ampicillin; 30 µg/ml chloramphenicol; 50 µg/ml kanamycin; 0.1-0.2% arabinose.

4.2 RNA and protein extraction

Cultures of KG-273, KG-276 or KG-289 were grown overnight in LD medium at 37 °C, diluted to OD_{600}= 0.1 in 120 ml of LD and grown up to OD_{600}= 0.4 at 28 °C. Aliquots were transferred in three flasks and incubated at different temperatures. 20 and 10 ml samples for protein extraction were taken after 20 and 60 min, chilled on ice and centrifuged at low speed to collect the cells. Pellets were washed with 10 mM Tris-HCl pH 7.5, centrifuged as above and frozen at -80°C for at least 60 min. The cell pellets were thawed in ice and resuspended in 500 µl of 10 mM Tris-HCl pH= 7.5. The cells were lysed by sonicating 3x 15 sec and then centrifuged at 8500 rpm for 5 min to eliminate non-lysed cells and gross cell debris. KG-276 and KG-289 total extracts were directly analysed by SDS-PAGE, whereas KG-273 total extracts were further processed as described [37] to collect membrane proteins. In both cases, samples were quantified by the Bradford assay [38] and their concentration adjusted to the same value. 15 µg protein samples were diluted 1:1 in protein loading sample buffer (50 mM Tris– HCl pH 6.8, 2% SDS, 0.1% bromophenol blue, and 10% glycerol) and loaded onto SDS-12% polyacrylamide gels. For mRNA half-life determination, 2 ml samples were taken for RNA extraction from cultures grown as described above and shifted at the different temperatures as indicated in Figure legends. Rifampicin (0.4 mg/ml final concentration)

was immediately added and 2 ml samples were taken at successive time points after the addition of the antibiotic for RNA extraction.

The intensities of Northern blotting signals determined with ImageQuant were plotted on a logarithmic scale over time. The half-life was calculated as $T_{1/2} = \ln2/k$, where k was the slope of the decay curve.

4.3 Protein stability determination

Cultures of KG-276 were grown at 28 °C up to OD_{600}= 0.4 and further incubated 20 min at 28 and 42 °C. Chloramphenicol (final concentration, 100 μg/ml) was added and 20 ml samples were taken for protein extraction immediately before and 45 and 90 min after the antibiotic addition. Protein extraction, SDS-PAGE and in-gel fluorescence imaging were performed as described above.

4.4 In-gel fluorescence determination

To detect fluorescent signals of LpxT-sfGFP, the gels were imaged after the run by means of a VersaDoc MP instrument using the Alexa Fluor 488 filter.

4.5 Western blotting hybridization

For immunological detection of proteins, after the run the gels were blotted onto PROTRAN nitrocellulose membranes (PerkinElmer) and the membranes stained with Ponceau S solution (Sigma). Immunodecoration was performed with one of the following antibodies diluted in Blotto (1% dried milk,50 mM Tris-HCl pH=7.5, 150 mM NaCl, 0.1% Triton X-100): i) polyclonal anti-GFP (A6455; Sigma); ii) polyclonal anti-LptC (kindly provided by A. Polissi).

4.6 Fluorescence assay

Cultures of BW25113 cultures carrying pGM2054 and derivatives were grown up to $OD_{600}= 0.4$ at 28 and 42 °C in LD with 30 µg/ml chloramphenicol. 1 ml samples were taken for fluorescence measurements. Cells were collected by centrifugation, washed, resuspended in cold PBS at $OD_{600}= 1.0$. After at least 1h incubation in ice, 100 µl cell samples were transferred in black polystyrene 96 well microplates and both fluorescence$_{485/535}$ ($F_{485/535}$) and OD_{600} were measured by means of an Ensight (PerkinElmer) microplate reader. GFP activity was expressed in arbitrary units (AU) as the ratio $F_{485/535}/OD_{600}$.

4.7 RNA analyses

Procedures for RNA extraction, *in vitro* transcription with T7 RNA polymerase, Northern blot analysis, staining of the RNA on filters with methylene blue and 5'-end labeling of oligonucleotides with [γ^{32P}]- ATP and T4 polynucleotide kinase were previously described [8]. Oligonucleotide probes used for Northern blotting were 3172 (GFP); 3258 (HA); 3388. The *lpxT*-specific riboprobe was obtained by *in vitro* transcription with T7 RNA polymerase and [α^{32P}] CTP of DNA fragments obtained by PCR amplification of 2268824-2268928 MG1655 genomic region (oligonucleotides 3259-3270).

The 5'-end of the *lpxT* mRNA was determined by primer extension as previously described [39] with the radiolabelled oligonucleotide 3245 on 20 µg of RNA extracted from cultures of BW25113 grown in LD. The same oligonucleotide was used for Sanger-sequencing of an amplicon obtained by PCR amplification of MG1655 DNA with primers 3210-3245 (region 2372914-2268928). The 5'-end of the mRNA produced by pLPXTp was mapped by primer extension with the oligo 3408 on 10 µg of RNA extracted from BW25113/pLPXTp. The sequencing ladder was obtained by Sanger sequencing of a PCR fragment amplified with primers 2804-3281 on pLPXTp DNA. Images of Northern blots and primer extension gels were obtained by phosphorimaging using ImageQuant

software (Molecular Dynamics). ImageQuant was used also for densitometric analyses of Northern and western blotting experiments.

RT-qPCR (Reverse Transcription-quantitative PCR) was performed on RNA extracted from four independent cultures for each strain at OD_{600}=0.4. 1 µg was reverse-transcribed with the Takara PrimeScript[TM] RT kit (Perfect Real Time) and a 1:100 cDNA dilution was used for Real-Time PCR with SYBR® Premix Ex Taq[TM] (Takara) and primers specific for either the GFP mRNA (primers 3506-3172) or 16S rRNA (used as reference gene; primers 3398-3399).

4.8 *In vitro* RNA decay

E. coli crude extracts were obtained as described [40] from exponential cultures of BW25113 grown at 28 and 42 °C, and of C-5869 (rne^+) and C-5868 (rne ts) grown at 28 °C. Protein content was determined using Bradford Reagent (Sigma). RNA degradosome was purified from cultures of the *E. coli* C-5602 (rne^+) strain grown at 37 °C as described [40]. Fraction 9 (see Fig. 6 of Reference [40]) was used in this work. ^{32}P-labelled LPXT riboprobe, which corresponds to the first 80 nt of the *lpxT* transcript (coordinates 2268826-2268905), was synthesized by *in vitro* transcription with T7 RNA polymerase and [α-^{32}P] CTP of a DNA fragment obtained by PCR with the oligonucleotides 3318-3332 on MG1655 chromosomal DNA. Protection of 3'-end was performed by heating a mixture of the LPXT riboprobe and a fivefold molar excess of the primer 3332 (T_M= 62.5 °C at [NaCl]= 50 mM; calculated with Oligo Calc: Oligonucleotide Properties Calculator [41]) at 95 °C and slowly cooling it to 42 °C. 70000 cpm of probe in Binding Buffer (50 mM Tris-HCl, pH 7.4, 50 mM NaCl, 0.5 mM DTT, 0.025 % NP40 (Fluka) and 10 % glycerol) was denatured at 90 °C for 2 min, preincubated at 28 or 42 °C for 10 min and incubated 10 min at 28 or 42 °C with 300 ng of crude extract in a final volume of 10 µl. Extracts of the C-5868 and C-5869 strains were pre-incubated 10 min at 44 °C before riboprobe addition to inactivate RNase E. Samples were extracted with phenol-chloroform, precipitated with ethanol and resuspended in 5 µl

of loading buffer (10 M urea, TBE 0.2X, EDTA 2mM, Xylene-cyanol 0.025%, Bromophenol Blue 0.025%). Degradation by RNA degradosome was assayed by incubating 16.5 ng of RNA degradosome with 70000 cpm of the ^{32}P-labelled LPXT-3332 oligonucleotide complex in 20 mM Tris-HCl, pH 7.5, 20 mM KCl, 1.5 mM DTT, 1 mM MgCl$_2$. Reactions were stopped by adding an equal volume of 2x loading buffer and heating 3 min at 95 °C.

4.9 Statistical analysis

Significance was evaluated with t-test or One-way ANOVA and post-hoc Tukey HSD analysis, as indicated in Figure legends.

5. ACKNOWLEDGMENTS

6. REFERENCES

[1]   T.J. Silhavy, D. Kahne, S. Walker, S. Chowdhury, C. Maris, F.H.-T. Allain, F. Narberhaus, C. Ragaz, E. Kreuger, F. Narberhaus, H. Nikaido, T.J. Silhavy, D. Kahne, S. Walker, F. Narberhaus, T. Waldminghaus, S. Chowdhury, M.A. Curtis, R.S. Percival, D. Devine, R.P. Darveau, S.R. Coats, M. Rangarajan, E. Tarelli, P.D. Marsh, M. El Ghachi, A. Derbise, A. Bouhss, D. Mengin-lecreulx, G.A. Mackie, M.B. Stead, A. Agrawal, K.E. Bowden, R. Nasir, B.K. Mohanty, R.B. Meagher, S.R. Kushner, X. Wang, P.J. Quinn, The bacterial cell envelope., Cold Spring Harb. Perspect. Biol. 2 (2010) a000414. doi:10.1101/cshperspect.a000414.

[2]   C.R.H. Raetz, C.M. Reynolds, M.S. Trent, R.E. Bishop, Lipid A modification systems in gram-negative bacteria., Annu. Rev. Biochem. 76 (2007) 295–329. doi:10.1146/annurev.biochem.76.010307.145803.

[3]   B.D. Needham, M.S. Trent, Fortifying the barrier: the impact of lipid A remodelling on bacterial pathogenesis., Nat. Rev. Microbiol. 11 (2013) 467–481. doi:10.1038/nrmicro3047.

[4]   Y. Li, D.A. Powell, S.A. Shaffer, D.A. Rasko, M.R. Pelletier, J.D. Leszyk, A.J. Scott, A. Masoudi, D.R. Goodlett, X. Wang, C.R.H. Raetz, R.K. Ernst, LPS remodeling is an evolved survival strategy for bacteria, Proc. Natl. Acad. Sci. 109 (2012) 8716–8721. doi:10.1073/pnas.1202908109.

[5]   K. Kawahara, H. Tsukano, H. Watanabe, B. Lindner, M. Matsuura, Modification of the structure and activity of lipid A in *Yersinia pestis* lipopolysaccharide by growth temperature, Infect. Immun. 70 (2002) 4092–4098 doi:10.1128/IAI.70.8.4092-4098.2002.

[6]   M.K. Ray, G.S. Kumar, S. Shivaji, Phosphorylation of lipopolysaccharides in the antarctic psychrotroph *Pseudomonas syringae*: A possible role in temperature adaptation, J. Bacteriol. 176 (1994) 4243–4249. doi: 10.1128/jb.176.14.4243-4249.1994

[7]   M.A. Curtis, R.S. Percival, D. Devine, R.P. Darveau, S.R. Coats, M. Rangarajan, E. Tarelli, P.D. Marsh, Temperature-dependent modulation of *Porphyromonas gingivalis* lipid A structure and interaction with the innate host defenses., Infect. Immun. 79 (2011) 1187–1193. doi:10.1128/IAI.00900-10.

[8]   F. Delvillani, B. Sciandrone, C. Peano, L. Petiti, C. Berens, C. Georgi, S. Ferrara, G. Bertoni, M.E.M.E. Pasini, G. Dehò, F. Briani, Tet-Trap, a genetic approach to the identification of bacterial RNA thermometers: application to *Pseudomonas aeruginosa*, RNA. 20 (2014) 1963–1976. doi:10.1261/rna.044354.114.

[9]   T. Touzé, A.X. Tran, J. V. Hankins, D. Mengin-Lecreulx, M.S. Trent, Periplasmic phosphorylation of lipid A is linked to the synthesis of undecaprenyl phosphate, Mol. Microbiol. 67 (2008) 264–277. doi:10.1111/j.1365-2958.2007.06044.x.

[10]   E.M. Nowicki, J.P. O'Brien, J.S. Brodbelt, M.S. Trent, Characterization of *Pseudomonas aeruginosa* LpxT reveals dual positional lipid A kinase activity and co-ordinated control of outer membrane modification, Mol. Microbiol. 94 (2014) 728–741. doi:10.1111/mmi.12796.

[11]   Z. Zhou, S. Lin, R.J. Cotter, C.R.H. Raetz, Lipid A modifications characteristic of *Salmonella typhimurium* are induced by NH_4VO_3 in *Escherichia coli* K12. Detection of 4-amino-4-deoxy-L- arabinose, phosphoethanolamine and palmitate, J. Biol. Chem. 274 (1999) 18503–18514. doi:10.1074/jbc.274.26.18503.

[12]   C.M. Herrera, J. V. Hankins, M.S. Trent, Activation of PmrA inhibits LpxT-dependent phosphorylation of lipid A promoting resistance to antimicrobial peptides, Mol. Microbiol. 76 (2010) 1444–1460. doi:10.1111/j.1365-2958.2010.07150.x.

[13]   L.D. Tatar, C.L. Marolda, A.N. Polischuk, D. van Leeuwen, M.A. Valvano, An *Escherichia coli* undecaprenyl-pyrophosphate phosphatase implicated in undecaprenyl phosphate recycling., Microbiology. 153 (2007) 2518–2529. doi:10.1099/mic.0.2007/006312-0.

[14]   A. Rath, M. Glibowicka, V.G. Nadeau, G. Chen, C.M. Deber, Detergent binding explains anomalous SDS-PAGE migration of membrane proteins, Proc. Natl. Acad. Sci. 106 (2009) 1760–1765. doi:10.1073/pnas.0813167106.

[15]   C.P. Corcoran, D. Podkaminski, K. Papenfort, J.H. Urban, J.C.D. Hinton, J. Vogel, Superfolder GFP reporters validate diverse new mRNA targets of the classic porin regulator, MicF RNA, Mol. Microbiol. 84 (2012) 428–445. doi:10.1111/j.1365-2958.2012.08031.x.

[16]   E.B. Gogol, V.A. Rhodius, K. Papenfort, J. Vogel, C.A. Gross, Small RNAs endow a transcriptional activator with essential repressor functions for single-tier control of a global stress regulon, Proc. Natl. Acad. Sci. 108 (2011) 12875–12880. doi:10.1073/pnas.1109379108.

[17]   X. Hong, H.D. Chen, E.A. Groisman, Gene expression kinetics governs stimulus-specific decoration of the *Salmonella* outer membrane., Sci. Signal. 11 (2018) eaar7921. doi:10.1126/scisignal.aar7921.

[18]   F. Repoila, S. Gottesman, Temperature sensing by the *dsrA* promoter., J. Bacteriol. 185 (2003) 6609–6614. doi: 10.1128/JB.185.22.6609-6614.2003

[19]   M.P. Hui, P.L. Foley, J.G. Belasco, Messenger RNA degradation in bacterial cells, Annu. Rev. Genet., 48 (2014), pp. 537-559. doi: 10.1146/annurev-genet-120213-092340

[20]   Y. Chao, L. Li, D. Girodat, K.U. Förstner, N. Said, C. Corcoran, M. Śmiga, K. Papenfort, R. Reinhardt, H.J. Wieden, B.F. Luisi, J. Vogel, *In Vivo* Cleavage Map Illuminates the Central Role of RNase E in Coding and Non-coding RNA Pathways, Mol. Cell. 65 (2017) 39–51. doi:10.1016/j.molcel.2016.11.002.

[21]   A.J. Carpousis, The RNA Degradosome of *Escherichia coli* : An mRNA-Degrading Machine Assembled on RNase E, Annu. Rev. Microbiol. 61 (2007) 71–87. doi:10.1146/annurev.micro.61.080706.093440.

[22]   F. Briani, T. Carzaniga, G. Dehò, Regulation and functions of bacterial PNPase., Wiley Interdiscip. Rev. RNA. 7 (2016) 241–58. doi:10.1002/wrna.1328

[23]   L. Davydova, S. Bakholdina, M. Barkina, P. Velansky, M. Bogdanov, N. Sanina, Effects of elevated growth temperature and heat shock on the lipid composition of the inner and outer membranes of *Yersinia pseudotuberculosis*, Biochimie. 123 (2016) 103–109. doi:10.1016/j.biochi.2016.02.004.

[24]   B. Schilling, J. Hunt, B.W. Gibson, M.A. Apicella, Site-specific acylation changes in the lipid A of *Escherichia coli lpxL* mutants grown at high temperatures, Innate Immun. 20 (2014) 269–282. doi:10.1177/1753425913490534.

[25]   R.K. Ernst, K.N. Adams, S.M. Moskowitz, G.M. Kraig, K. Kawasaki, C.M. Stead, M.S. Trent, S.I. Miller, The *Pseudomonas aeruginosa* lipid A deacylase: selection for expression and loss within the cystic fibrosis airway., J. Bacteriol. 188 (2006) 191–201. doi:10.1128/JB.188.1.191-201.2006.

[26]   A. Ishihama, Functional Modulation of *Escherichia coli* RNA Polymerase , Annu. Rev. Microbiol. 54 (2002) 499–518. doi:10.1146/annurev.micro.54.1.499.

[27]   A. Coornaert, A. Lu, P. Mandin, M. Springer, S. Gottesman, M. Guillier, MicA sRNA links the PhoP regulon to cell envelope stress, Mol. Microbiol. 76 (2010) 467–479. doi:10.1111/j.1365-2958.2010.07115.x.

[28]   A. Kato, H.D. Chen, T. Latifi, E.A. Groisman, Reciprocal Control between a Bacterium's Regulatory System and the Modification Status of Its Lipopolysaccharide, Mol. Cell. 47 (2012) 897–908. doi:10.1016/j.molcel.2012.07.017.

[29]   J.M. Froelich, K. Tran, D. Wall, A *pmrA* constitutive mutant sensitizes *Escherichia coli* to deoxycholic acid, J. Bacteriol. 188 (2006) 1180–1183. doi:10.1128/JB.188.3.1180-1183.2006.

[30]   E.J. Rubin, C.M. Herrera, A.A. Crofts, M.S. Trent, PmrD is required for modifications to *Escherichia coli* endotoxin that promote antimicrobial resistance, Antimicrob. Agents Chemother. 59 (2015) 2051–2061. doi:10.1128/AAC.05052-14.

[31]   E.M. Nowicki, J.P. O'Brien, J.S. Brodbelt, M.S. Trent, Extracellular zinc induces phosphoethanolamine addition to *Pseudomonas aeruginosa* lipid A via the ColRS two-component system, Mol. Microbiol. 97 (2015) 166–178. doi:10.1111/mmi.13018.

[32]   K.A. Datsenko, B.L. Wanner, One-step inactivation of chromosomal genes in *Escherichia coli* K-12 using PCR products., Proc. Natl. Acad. Sci. U. S. A. 97 (2000) 6640–6645. doi:10.1073/pnas.120163297.

[33]   M. Raneri, B. Sciandrone, F. Briani, A whole-cell assay for specific inhibitors of translation initiation in bacteria., J. Biomol. Screen. 20 (2015) 627–633. doi:10.1177/1087057114566376.

[34]   M. El Ghachi, A. Derbise, A. Bouhss, D. Mengin-Lecreulx, Identification of multiple genes encoding membrane proteins with undecaprenyl pyrophosphate phosphatase (UppP) activity in *Escherichia coli*, J. Biol. Chem. 280 (2005) 18689–18695. doi:10.1074/jbc.M412277200.

[35]   M. Lessl, D. Balzer, R. Lurz, V.L. Waters, D.G. Guiney, E. Lanka, Dissection of IncP conjugative plasmid transfer: Definition of the transfer region Tra2 by mobilization of the Tra1 region *in trans*, J. Bacteriol. 174 (1992) 2493–2500. doi: 10.1128/jb.174.8.2493-2500.1992

[36]   F. Briani, E. Del Vecchio, D. Migliorini, E. Hajnsdorf, P. Régnier, D. Ghisotti, G. Dehò, RNase E and polyadenyl polymerase I are involved in maturation of CI RNA, the P4 phage immunity factor, J. Mol. Biol. 318 (2002) 321–331. doi:10.1016/S0022-2836(02)00085-2.

[37]   S. Sandrini, R. Haigh, P. Freestone, Fractionation by Ultracentrifugation of Gram Negative Cytoplasmic and Membrane Proteins, Bio-Protocol. 4 (2014) 12–15. doi:dx.doi.org/10.21769/BioProtoc.1287.

[38]   M.M. Bradford, A rapid and sensitive method for the quantitation of microgram quantities of protein using the principle of protein dye binding, Anal. Biochem. 72 (1976) 248–254. doi:10.1016/0003-2697(76)90527-3.

[39]   F. Forti, P. Sabbattini, G. Sironi, S. Zangrossi, G. Dehò, D. Ghisotti, Immunity determinant of phage-plasmid P4 is a short processed RNA., J. Mol. Biol. 249 (1995) 869–878. doi:10.1006/jmbi.1995.0344.

[40]   M.E. Regonesi, F. Briani, A. Ghetta, S. Zangrossi, D. Ghisotti, P. Tortora, G. Dehò, A mutation in polynucleotide phosphorylase from *Escherichia coli* impairing RNA binding and degradosome stability., Nucleic Acids Res. 32 (2004) 1006–17. doi:10.1093/nar/gkh268.

[41]   W.A. Kibbe, OligoCalc: An online oligonucleotide properties calculator, Nucleic Acids Res. 35 (2007) W43-W46. doi:10.1093/nar/gkm234.

[42]   P. Sperandeo, F.K. Lau, A. Carpentieri, C. De Castro, A. Molinaro, G. Dehò, T.J. Silhavy, A. Polissi, Functional analysis of the protein machinery required for transport of lipopolysaccharide to the outer membrane of *Escherichia coli*, J. Bacteriol. 190 (2008) 4460–4469. doi:10.1128/JB.00270-08.

[43]   T. Carzaniga, F. Briani, S. Zangrossi, G. Merlino, P. Marchi, G. Dehò, Autogenous regulation of *Escherichia coli* polynucleotide phosphorylase expression revisited., J. Bacteriol. 191 (2009) 1738–48. doi:10.1128/JB.01524-08.

[44]   F.R. Blattner, The Complete Genome Sequence of *Escherichia coli* K-12, Science (80-.). 277 (1997) 1453–1462. doi:10.1126/science.277.5331.1453.

[45]   T. Carzaniga, D. Antoniani, G. Dehò, F. Briani, P. Landini, The RNA processing enzyme polynucleotide phosphorylase negatively controls biofilm formation by repressing poly-N-

acetylglucosamine (PNAG) production in *Escherichia coli* C., BMC Microbiol. 12 (2012) 270. doi:10.1186/1471-2180-12-270.

7. FIGURE LEGENDS

Fig. 1. LpxT expression at different temperatures. Cultures of strains expressing *lpxT-GFP* (KG273; A) or *lpxT-sfGFP* (KG276; B and C) were grown at 28°C up to $OD_{600}=0.4$ and proteins extracted after incubation at the temperatures indicated in the panels as detailed in Materials and Methods. A. Western blotting of membrane proteins (15 μg) run in an 12% polyacrylamide- 0.1% SDS gel and blotted onto a nitrocellulose filter. Proteins extracted from cultures of BW25113 (*lpxT*[+]) were analysed as negative control. Filters were immunodecorated with GFP (upper panel) and LptC (lower panel) specific antibodies. LptC is an inner membrane protein [42] and was used as gel loading control. The position of MW markers on the filter is reported on the left of the panels. The numbers below the lanes refer to quantification with ImageQuant of $LpxT_{GFP}$ signals normalized for LptC signals and for the value obtained for the reference condition (i.e. 20 min incubation at 28 °C). na, not applicable. B and C. LpxT-sfGFP amount in total cell extracts as estimated by in-gel fluorescence. B. Samples for protein extraction were taken after 20 (not shown) and 60 min acclimation at the temperatures indicated below the bars. $LpxT_{sfGFP}$ signals were quantified by densitometry with ImageQuant and values were normalized for the value of the reference condition. The columns represent the average of at least three determinations with standard deviation. Significance was evaluated with One-way ANOVA and Tukey HSD (α=0.05; *, $P<0.05$; **, $P<0.01$; ***, $P<0.001$). N.F., Normalized Fluorescence. C. Samples for protein extraction were taken immediately before (0) and 45 and 90 min after chloramphenicol addition (final concentration, 100 μg/ml) to exponential cultures of KG276 acclimated 20 min at 28 and 42 °C. The experiment was repeated three times with similar results. Upper panel, in-gel fluorescence imaging; lower panel, gel stained with Ponceau S solution (Sigma) as loading control.

Fig. 2. *lpxT* transcription at different temperatures A. Mapping of the 5'-end of *lpxT* mRNA. Primer extension was performed with the radiolabelled oligo 3245 on 20 µg of RNA extracted from exponential (E) or stationary (S) cultures of BW25113 grown at 28 °C. The same primer was used for Sanger-sequencing of a PCR fragment amplified on genomic DNA with the oligonucleotides 3210-3245. The coordinate of the identified 5'-end (position 2268826 of Genbank Accession Number U00096.3) is reported beside the panel. B and C. Expression and stability of *lpxT* (B and C) and *lpxT*-GFP (D) mRNAs. Samples for RNA extraction were taken from exponential cultures of BW25113 (*lpxT*) or KG273 (*lpxT*-GFP) grown at 28 °C up to OD_{600}=0.4 and incubated 15 min at different temperatures. Samples were taken at the time points indicated in min above the lanes before (0) or after the addition of rifampicin to block transcription initiation. 20 µg of RNA were run in 1.2% denaturing agarose gels, blotted onto a nylon filter and hybridized with the *lpxT*-specific radiolabeled riboprobe. 16S rRNA (16S) stained with methylene blue after transfer is shown as loading control. The position and MW (in kb) of bands of the RiboRuler™ High Range RNA ladder (Thermo Scientific) is reported on the left. The results are representative of three experiments performed in the same conditions. B. Signals obtained before rifampicin addition in three replicate experiments were quantified with ImageQuant. Bars represent average with standard deviation. Significance (*, P<0.05; **, P<0.01; ns, not significant) was evaluated with ANOVA and Tukey HSD test.

Fig. 3. Identification and activity of *lpxTp* promoter. A. *lpxTp*-GFP transcriptional fusions. The region inserted in pLPXTp and pLPXTpmut is reported in grey. Numbers refer to relative position respect to the *lpxT* mRNA TSS (+1, position 2268826). The bases differing in the two constructs are in italics (TA*AGG*T, pLPXTp; TA*TAA*T, pLPXTpmut). In green, the GFP reporter gene with the 55 bp long *recA* 5'-UTR carried by the plasmid vector. B. Fluorescence of cultures of BW25113 carrying the indicated plasmids. Vector, pGM2054. The cultures were grown at 28 °C (light grey

bars) and 42 °C (dark grey bars) and fluorescence measured as detailed in Materials and Methods. Fluorescence values were normalized by the average fluorescence of the negative control (BW25113/pGM2054 at 28 °C). The bars represent average (n=3) with standard deviation. Significance (P) calculated by T-test is reported. C. 10 μg of RNA extracted from BW25113/pLPXTp cultures in exponential (E) and stationary (S) phase were analysed by primer extension with the oligonucleotide 3408. The sequencing ladder was obtained by Sanger sequencing with the same primer of a PCR fragment amplified with oligonucleotides 2804-3281 on pLPXTp DNA. The star indicates the 5'-end of the *recA*-GFP mRNA transcribed from the plasmid. D. Relative amount of GFP mRNA. RNA extracted from cultures of BW25113 carrying either plasmid pLPXTp (TAAGGT) or pLPXTpmut (TATAAT) grown up to OD_{600}=0.4 at 28 °C and acclimated for 1h at 28 or 42 °C was analysed by RT-qPCR. The bars (light and dark grey, 28 and 42 °C, respectively) represent average (n=4) with standard deviation of the relative amount (R.A.) of GFP mRNA calculated by normalizing all values for the lowest value obtained at 28 °C. Significance (P) calculated by T-test is reported. ns, not significant.

Fig. 4. *lpxT* mRNA decay at different temperatures. A. Scheme of pLPXT and pLPXTHA constructs (not represented on scale). Bent arrow, *araBp* promoter; boxes, *lpxT* and *lpxT*-HA ORFs; continuous lines, *lpxT* 5'- and 3'-UTRs; dotted lines, vector. B, C and D. Cultures of BW25113/pLPXT (B), BW25113/pLPXTHA (C), C-5868 (*rne-131*)/pLPXT and C-5869 (*rne$^+$*)/pLPXT were grown at 28 °C up to OD_{600}=0.4, split in two and incubated 10 min with 0.1% arabinose at either 28 or 42 °C. Rifampicin (0.4 mg/ml) was added and samples for RNA extraction were taken immediately before (t=0) and at the time points after the addition indicated above the lanes. 10 μg of RNA were run in a 5% polyacrylamide-urea gel, blotted onto a nylon filter and hybridized with the 3388 (B and D) or HA-specific (C) oligonucleotides. In the lower panels, tRNAs stained with ethidium bromide before blotting as gel loading control are shown. The mRNA half-life (HL) estimated on triplicate cultures is reported in min with standard deviation below the tRNA panels. B, left panel. The position and MW (in kb) of bands of the RiboRuler™ Low Range

RNA ladder (Thermo Scientific) is reported. B, right panel. Signals were quantified with ImageQuant and normalized for signals obtained at 28 °C at t=0. The average values obtained in three replicate experiments were plotted *vs*. time. Error bars, standard deviation; dotted lines, trendlines; empty symbols, RNA extracted from cultures at 28 °C; black symbols, RNA extracted from cultures at 42 °C. D, only RNA samples extracted from cultures acclimated at 42 °C are shown.

Fig. 5. *In vitro* degradation of LPXT probe. A.70000 cpm of uniformly radiolabeled LpxT probe were incubated 10 min at the temperature indicated above the lanes (T_i) without (lower panel) or with 300 ng of crude extracts of BW25113 (upper panel). T_e, temperature at which the cultures for extract preparation were grown; FL, full length probe; NI, not incubated. Samples were run in a 6% denaturing polyacrylamide minigel (upper part) or a 6% denaturing polyacrylamide sequence gel (lower panel). B. The uniformly radiolabeled LpxT probe (70000 cpm) annealed with the 3332 oligonucleotide was incubated 10 min at 42 °C without (-) or with 300 ng of crude extracts of BW25113 (B, *rne*$^+$), C-5869 (+; *rne*$^+$) or C-5868 (ts; *rne* ts). The size of the full length probe and of the a degradation fragment is indicated in nt on the right. C. 70000 cpm of radiolabeled LpxT-3332 complex were incubated with 16.5 ng of RNA degradosome. Samples were taken at the time indicated above the lanes. The numbers below the lanes indicate the fraction of full length probe remaining with respect to time= 0 estimated by densitometry of the signals with ImageQuant. The position and MW (in nt) of radiolabeled DNA oligonucleotides used as MW markers is reported on the right. FL, full length probe. B and C. Samples were run in a 6% denaturing polyacrylamide sequence gel.

Table 1. Bacterial strains and plasmids

Strain	Relevant Genotype	Origin or reference
BW25113	$lpxT^+ rne^+$	[32]
C-5602	rne^+	[40]
C-5868	rne-131:Tn10	[43]
C-5869	rne^+:Tn10	[43]
DMEG3	BW25113 Δ$lpxT$:cat	[34]
KG-273	BW25113 $lpxT$-GFP	this work
KG-276	BW25113 $lpxT$-sfGFP	this work
KG-279	BW25113 Δ$lpxT$	this work
KG-280	KG-279 Δ$araB$::[$lpxT$-sfGFP:cat]	this work
KG-283	KG-279 Δ$araB$::[sfGFP:cat]	this work
KG-289	KG-276 Δ$micA$:$tetR$	this work
MG1449	Δ$micA$:$tetR$	[27]
MG1655		[44]

Plasmids and phage	Relevant characteristics[a]	Reference
pGM930	pBAD24-Δ1 [45] derivative with the insertion of t_Ω region	[8]
pGM931	pHERD20T derivative carrying $araBp$-t_Ω region of pGM930	[8]

pGM963	carries the eGFP gene	[33]
pGM2011	pGM931 derivative with the insertion of sfGFP	[8]
pGM2016	pGM2011 derivative, carries *recA* (2334354-2334277) translationally fused to sfGFP.	[8]
pGM2032	pGM2011 derivative, carries *lpxT* (2268742-2268859) translationally fused to sfGFP	This work
pGM2035	pGM930 derivative, carries the HA epitope coding region downstream of the *araBp* promoter	This work
pGM2040	pGZ119EH derivative, carries the *recA-sfGFP* reporter gene between *EcoR*I and *Pst*I sites	This work
pGM2049	pGM2035 derivative, carries *recA-lpxT* (regions 1020995-1020975 + 2268846-2269564) translationally fused to the HA region	This work
pGM2054	pGM2040 derivative, deletion of the region between *EcoR*V and *EcoR*I	This work
pGM2096	pGM930 derivative, carries *lpxT* (2268826-2269564) translationally fused to the sfGFP	This work
pGM2107	pGM2096 derivative, carries the *cat* gene inserted into the *Sma*I site	This work
pGM2109	pGM2016 derivative, carries the *cat* gene inserted into the *Sma*I site	This work
pGZ119HE	*oriV ColD*; CamR	[35]
pKD3	carries the *cat* gene	[32]
pKD13	carries the *kanR* gene	[32]
pKD46	carries λ RED recombination genes	[32]

pLPXT	pGM930 derivative, carries the *lpxT* gene (2268826-2269744)	This work
pLPXTHA	pGM2035 derivative, carries *lpxT* (2268826-2269564) translationally fused to the HA region	This work
pLPXTp	pGM2040 derivative, carries the region 2268778-2268826 between *EcoR*V and *EcoR*I restriction sites	This work
pLPXTpmut	pLPXTp derivative, carries the substitution of the 2268815-2268817 AGG region with TAA	This work
pXG-10SF	carries the sfGFP gene	[15]

[a] *E. coli* coordinates refer to Genbank Accession Number U00096.3.

Table 2.

lpxT mRNA half-life

Strain	Allele	Replicon[a]	mRNA half-life (min)	
			28 °C	42 °C
BW25113	*lpxT*+	Chr	3.9±0.6[b]	na
KG-273	*lpxT*-GFP	Chr	3.7±0.3[b]	na
BW25113/pLPXT	*lpxT*+	PLS	3.1±0.9[b]	1.1±0.2[b]
C-5868 (*rne ts*)/pLPXT	*lpxT*+	PLS	nt	3.0±0.8[b]
C-5869 (*rne*+)/pLPXT	*lpxT*+	PLS	4.3±0.4[c]	1.1±0.6[b]
BW25113/pLPXTHA	*lpxT*-HA	PLS	>4.0[b]	1.7±0.5[b]

1

C

[a]Chr, chromosomal *lpxT* gene; PLS, *lpxT* gene carried by the plasmid
[b]mRNA half-life was estimated as described in Materials and Methods and Fig. 4B legend on triplicate cultures. Average with standard deviation is reported. na, not applicable; nt, not tested.
[c]Average with range of mRNA half-life estimated in two replicate experiments.
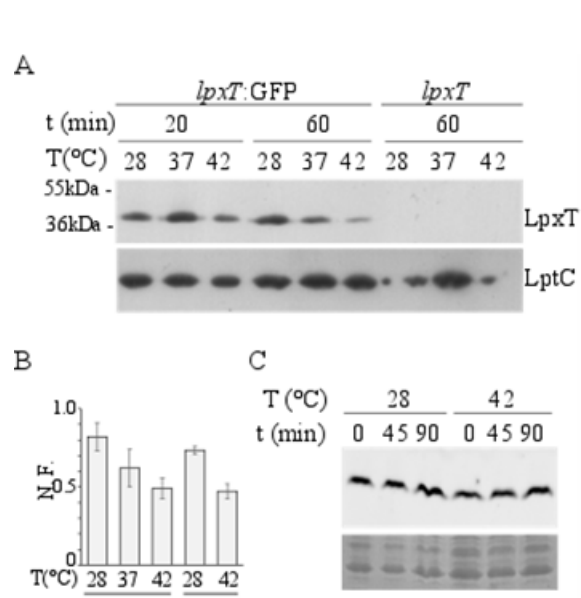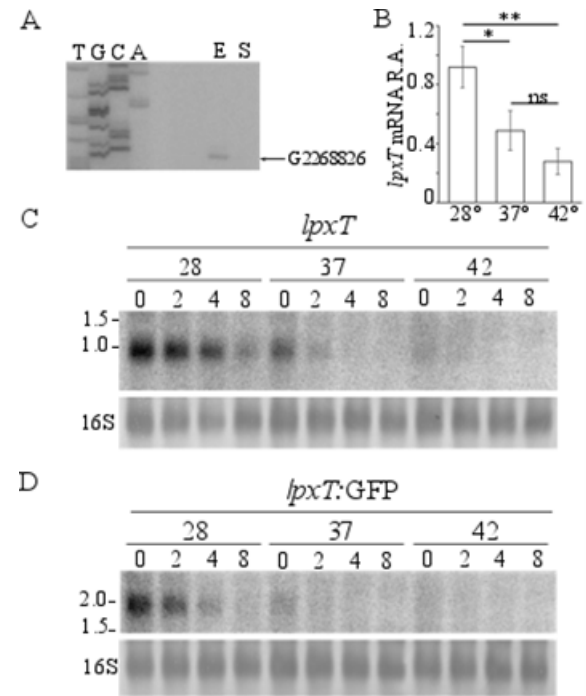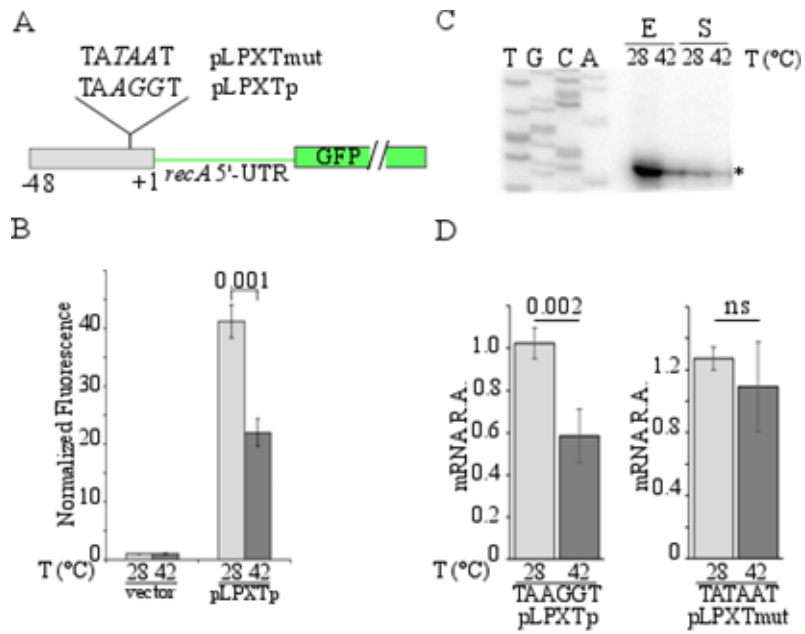
A

lpxT:GFP   *lpxT*

t (min)   20   60   60
T(°C)   28 37 42   28 37 42   28 37 42
55kDa -
36kDa -   LpxT

                                                         LptC

B   C
                       T (°C)   28   42
                       t (min) 0 45 90   0 45 90

N.F.

T(°C) 28 37 42 28 42

Fig. 1

A

T G C A   E S

                                    — G2268826

B

lpxT mRNA R.A.

28° 37° 42°

C   *lpxT*

              28   37   42
         0 2 4 8   0 2 4 8   0 2 4 8

1.5-
1.0-

16S

D   *lpxT*:GFP

              28   37   42
         0 2 4 8   0 2 4 8   0 2 4 8
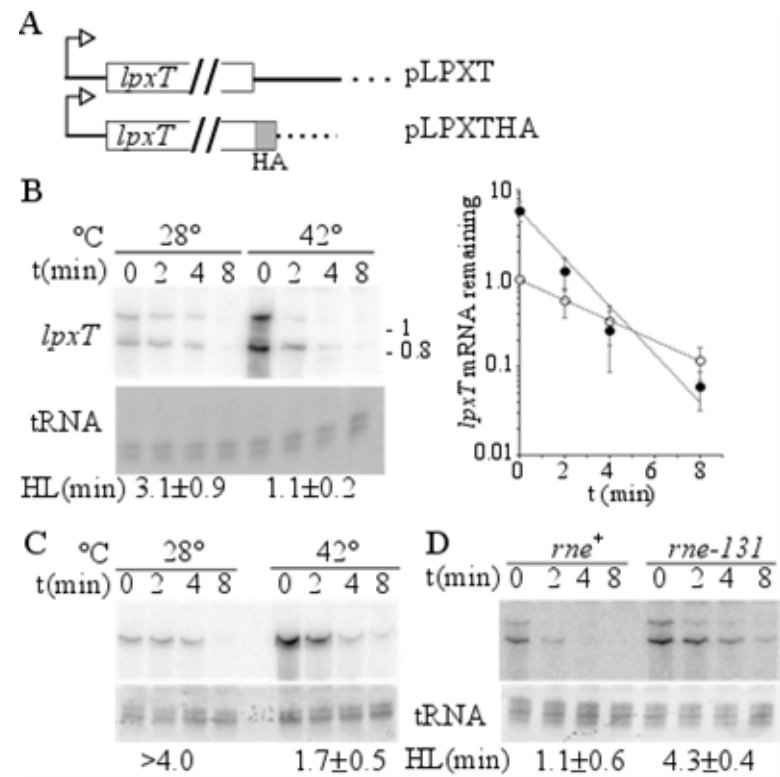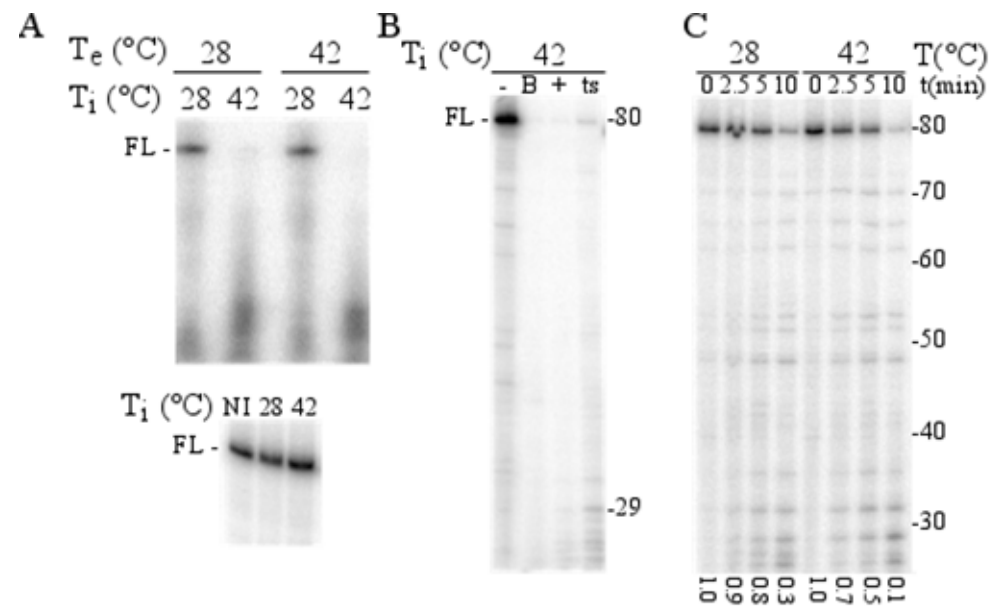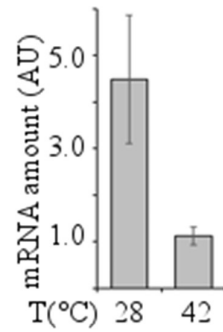
2.0-
1.5-

16S

Sciandrone et al., Fig. 2

Fig. 3

Fig. 4

Sciandrone et al., Fig. 5

SUPPLEMENTARY FIGURES

Supplementary Fig. S1. *lpxT* expression in the acclimation phase to high temperature. Samples for RNA extraction were taken from exponential cultures of BW25113 grown at 28 °C up to OD_{600}=0.4 and incubated 5 min at 28 or 42 °C. 20 μg of RNA were run in 1.5% denaturing agarose gels, blotted onto a nylon filter and hybridized with the *lpxT*-specific radiolabeled riboprobe. Signals corresponding to *lpxT* mRNA were quantified with ImageQuant software. Bars represent average with range of the results of densitometric analysis obtained in two independent experiments. AU, arbitrary units.
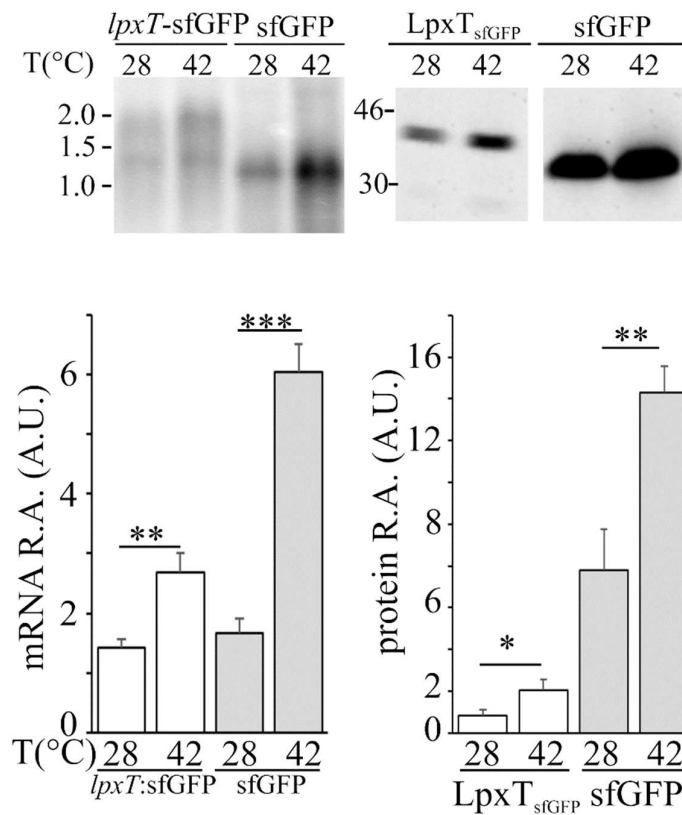
Supplementary Fig. S2. Expression at different temperatures of reporter constructs inserted into the _araB_ locus. Samples for RNA and protein extraction were taken from exponential cultures of KG-280 (_lpxT_-sfGFP) and KG-283 (sfGFP) grown at 28 °C up to OD_{600}=0.4, induced for 30 min with 0.1% arabinose and further incubated 15 min at 28 or 42 °C. Left panel. 20 µg of RNA were run in 1.5% denaturing agarose gels, blotted onto a nylon filter and hybridized with the GFP-specific radiolabeled oligonucleotide. The position and MW (in kb) of size markers is shown on the left. Right panel. 13 µg of total proteins were run in 15% denaturing polyacrylamide gels and signals of fluorescent proteins acquired with a Versadoc instrument. The position and MW (in kDa) of size markers is shown on the left. Radioactive and fluorescent signals were quantified with ImageQuant software and values were normalized for the value of the reference condition (KG-280 at 28 °C). The columns represent the average of three determinations with standard deviation. Significance (P) calculated by T-test is reported (*, P<0.05; **, P<0.01; ****, P<0.001). AU, arbitrary units.

A. LPXT probe and predicted secondary structure of the *lpxT* 5'-UTR

<u>GUUUU</u>UCAGUAAGAUAAUUAGAGAAAAUaugAUUAA<u>AAAUU</u>UGCCGCAAAUAGUG
UUGUUGA<u>AUAUU</u>GUCGGCCUCGCGC
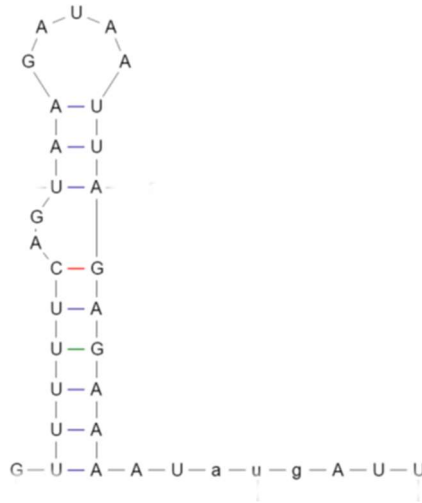
B. *lpxTp* promoter

Pa CGCTACGAATGAGGGA<u>ATGACA</u>AGTGAGTGACAAAGGCC<u>TATAAA</u>AGCGC**G**

Ec GAGCGCGCTGTTGAAGCTTCGTTTAGCGACTACCGCG<u>TAAGGT</u>TGCCTGC**G**

Supplementary Fig. S3. Sequence of the *lpxT* mRNA 5'-end and of *P. aeruginosa* and *E. coli* *lpxT* promoter regions. A, upper part. The sequence of the LPXT riboprobe, corresponding to the first 80 nt of *lpxT* mRNA, is reported. In lowercase, the AUG start codon. Underlined, regions with putative RNase E cleavage sites. A, lower part. Secondary structure of the *lpxT* mRNA 5'-end predicted with mfold [1]. B. The sequence of the 50 bp long region located immediately upstream of the *lpxT* gene TSS (boldface) in *P. aeruginosa* (Pa) and *E. coli* (Ec) is shown. The -10 and -35 regions are underlined; the putative PhoP binding site is boxed.

[1]   M. Zuker, Mfold web server for nucleic acid folding and hybridization prediction, Nucleic Acids Res. 31 (2003) 3406–3415. doi:10.1093/nar/gkg595.

Supplementary Table S1. Oligonucleotides

Name	Sequence[a]
1669	GTGTAGGCTGGAGCTGCTTC
2804	CTCCTGCAGCTATTTGTATAGTTCATCCATGC
3172	GACAAGTGTTGGCCATGGAAC
3210	GGGGTACCTTTCCAGCAGCGAAGCTG
3225	GGGCCATGGTTTTTCAGTAAGATAATTAGAG
3245	GGGGATATACCAGGAAAGAAAC
3257	CGAATTCTACCCATACGATGTTCCAGATTACGCTTGACTGCA
3258	GTCAAGCGTAATCTGGAACATCGTATGGGTAGAATTCGGTAC
3259	GCGTTTTTCAGTAAGATAATTAGAG
3270	**TAATACGACTCACTATAG**GGGGGGATATACCAGGAAAGAAAC
3273	GGAATTCTTTGTTTTGGAAATGTTTGTTTTTTC
3274	GGAATTCCAACAGAACATATTGACTATCC
3281	ATCGCGCGCTGTTGAAGCTTC
3282	GGAATTCGCAGGCAACCTTACGCG
3286	GGGCCATGGTATTACCCGGCATGACAGGAGAAAATATGATTAAAAATTTGCCGC
3318	**CTAATACGACTCACTATAG**GTTTTTCAGTAAGATAATTAGAGAAAATA
3332	GCGCGAGGCCGACAATATTC
3358	CCAGAGTAATGATTGGCGCACAC
3359	TTTGTTTTGGAAATGTTTGTTTTTTCCTGG
3360	GGAAAAAACAAACATTTCCAAAACAAAAGTAAAGGAGAAGAACTTTTCAC
3362	CCCTGATGATGTTAATTACTGTGAGCTGTCAAACATGAGAATTAATTCCG
3363	CTCACAGTAATTAACATCATCAGGG
3364	CAGAAAGTTAATAAGCGGGGTTGG
3373	GAAGCAGCTCCAGCCTACACCTGCAGCTATTTGTATAGTTCAT
3374	ATGAACTATACAAATAGCTGCAGGTGTAGGCTGGAGCTGCTTC
3388	GGGGTACCCGGCAAATTTTTAATCATATTTTC
3398	TGTCGTCAGCTCGTGTCGTGA

3399   ATCCCCACCTTCCTCCGGT

3408   CCAGTGAAAAGTTCTTCTCCTTTAC

3460   CCTTTTTTGACAAATCACTACCAGGAAAAAACAAACATTTCCAAAACAAAG
        CTGGCTCCGCTGCTGGT

3461   GCTCCAGCCTACACTTATTTGTAGAGCTCATCCATGCC

3462   GCTCTACAAATAAGTGTAGGCTGGAGCTGCTTC

3463   AGGATTATCCTCACTATAAAAATAACCCTGATGATGTTAATTACTGTGAGA
        TTCCGGGGATCCGTCGAC

3473   GGGAAGCTTGTGATACAGAAGTTAATAAGC

3475   GTGATTATTGGTCTGGTCATGC

3476   CCCGTCTCGAATTGGCTAGCGGATCCGCTGG

3477   GGCCCAGTCTTTCGACTGAG

3506   CTGTCCGTGGAGAGGGTG

3560   GGGCCGTGGGAATGGACCAGAACGCCGGGCATTTGCGCTGCATCGATACC
        CATATGAATATCCTCCTTA

3585   **CTAATACGACTCACTATAG**GGTATTACCCGGCATGACAGGAGAAAATA

ª Boldface characters, T7 promoter